1142–1154 *Nucleic Acids Research, 2011, Vol. 39, No. 3* *Published online 21 September 2010*
doi:10.1093/nar/gkq835

Optimizing anti-gene oligonucleotide 'Zorro-LNA' for improved strand invasion into duplex DNA

Eman M. Zaghloul[1,*], Andreas S. Madsen[2], Pedro M. D. Moreno[1], Iulian I. Oprea[1,3], Samir El-Andaloussi[1], Burcu Bestas[1], Pankaj Gupta[2], Erik B. Pedersen[2], Karin E. Lundin[1], Jesper Wengel[2] and C. I. Edvard Smith[1,*]

[1]Department of Laboratory Medicine, Karolinska Institutet, 141 86 Huddinge, Stockholm, Sweden, [2]Nucleic Acid Centre, Department of Physics and Chemistry, University of Southern Denmark, Denmark and [3]Department of Pharmaceutical Technology and Biopharmaceutics, Iuliu Hatieganu University of Medicine and Pharmacy, 400023 Cluj-Napoca, Romania

Received April 23, 2010; Revised September 3, 2010; Accepted September 6, 2010

ABSTRACT

Zorro-LNA (Zorro) is a newly developed, oligonucleotide (ON)-based, Z-shaped construct with the potential of specific binding to each strand of duplex DNA. The first-generation Zorros are formed by two hybridized LNA/DNA mixmers (2-ON Zorros) and was hypothesized to strand invade. We have now established a method, which conclusively demonstrates that an LNA ON can strand invade into duplex DNA. To make Zorros smaller in size and easier to design, we synthesized 3′–5′–5′–3′ single-stranded Zorro-LNA (ssZorro) by using both 3′- and 5′-phosphoramidites. With ssZorro, a significantly greater extent and rate of double-strand invasion (DSI) was obtained than with conventional 2-ON Zorros. Introducing hydrophilic PEG-linkers connecting the two strands did not significantly change the rate or extent of DSI as compared to ssZorro with a nucleotide-based linker, while the longest alkyl-chain linker tested (36 carbons) resulted in a very slow DSI. The shortest alkyl-chain linker (3 carbons) did not reduce the extent of DSI of ssZorro, but significantly decreased the DSI rate. Collectively, ssZorro is smaller in size, easier to design and more efficient than conventional 2-ON Zorro in inducing DSI. Analysis of the chemical composition of the linker suggests that it could be of importance for future therapeutic considerations.

INTRODUCTION

Silencing of gene expression has enormous implications for the treatment of genetic disorders especially for diseases with dominant inheritance (1). Gene silencing can be achieved either via the antisense mechanism, which acts on the mRNA level and prohibits mRNA translation (2), or via the anti-gene mechanism that directly targets the chromosomal DNA (3). While antisense therapy has shown great success through many strategies including single-stranded (ss) antisense oligonucleotides (ON), siRNA and ribozymes (4–7), the anti-gene technology remains significantly less explored (8). There are several barriers that greatly hamper the success of anti-gene agents. Anti-gene drugs must cross both the plasma membrane of cells as well as the nuclear membrane, and subsequently find their way through chromatin in order to recognize and specifically bind to their target sequences within the chromosomal DNA.

Many studies have aimed at optimizing anti-gene ON-based therapeutics (9). It has been shown that triplex-forming ONs (TFOs) are able to recognize the major groove of double-stranded (ds) DNA and interfere with initiation and elongation of gene transcription (10–13). However, TFOs are only able to target stretches of polypurines/polypyrimidines (14–16). Moreover, the Hoogsteen mechanism of binding, through which TFOs are working, is considered weak and can be interrupted by the nucleotide excision repair machinery in the cell (17,18). Therefore, agents that bind via Watson–Crick hybridization mechanisms constitute appealing alternatives. However, in order to efficiently bind to duplex DNA, improved non-natural nucleotide chemistries are needed.

Locked nucleic acid (LNA)-based ONs bind ssDNA efficiently through Watson–Crick mode. LNA is a class of nucleic acid analogues (19–21) containing a bridging methylene between the 2′-O and 4′-C of the ribose ring. The resulting conformationally restricted, bicyclic moiety leads to higher thermal stability of duplexes formed with

*To whom correspondence should be addressed. Tel: +46 8 58583663; Fax: +46 8 58583650; Email: eman.zaghloul@ki.se
Correspondence may also be addressed to C. I. Edvard Smith. Tel: +46 8 58583651; Fax: +46 8 58583650; Email: edvard.smith@ki.se

complementary DNA and RNA sequences. Over the last few years, some LNA-based therapeutics have been developed by the pharmaceutical industry. LNA/DNA mixmers have been frequently used as antisense drugs directed against RNA (22–27) and an interesting example of that is the 16-mer LNA-based drug 'SPC3042' showing high potency for survivin mRNA inhibition in the treatment of cancer (28). LNA ONs have also been successfully exploited in altering splicing both in cell cultures (29) and in mouse models (30). Moreover, four LNA antisense drugs are currently tested in human clinical trials as novel medicines against solid tumors, cancers of the blood and hepatitis C viral infection (http://www.santarispharma.com). On the other hand, there are no trials using LNA ONs as anti-gene drugs. LNA ONs have been utilized as anti-gene agents in cell cultures (31–35), but in none of these reports the actual mechanism of LNA binding was conclusively demonstrated. Thus, it is unclear whether strand invasion is the way by which these constructs hybridize to dsDNA.

Recently, we have generated a novel LNA-based, sequence-specific, anti-gene drug 'Zorro- LNA' (33,34). In the original design this agent consists of two LNA/DNA mixmer ONs attached to each other through a 7-nucleotide (7-nt), complementary linker region. One of the ONs is constructed to bind to the coding strand of DNA and the other to the template strand. We observed that Zorro-LNA (Zorro) can successfully bind to DNA duplexes and inhibit gene transcription on the plasmid level. Moreover, when Zorro was microinjected into cells stably transfected with the target site-containing reporter gene, it also mediated blocking of gene expression. We anticipated that 'double-strand invasion' is the mechanism by which Zorro binds to duplex DNA. However, this was never proven experimentally and for technical reasons the quantification of the amount of Zorro bound to DNA was not very precise.

Advantageously, and opposite to TFOs, Zorro-LNA does not seem to display any sequence restriction. However, avoiding intra-molecular binding between bases in the linker region and bases in the arms remained an obstacle making the design of the first-generation Zorro-LNAs a cumbersome process. Moreover, similar to siRNAs a preannealing step was required for the hybridization of the two ONs in order to generate the complete Zorro construct. For an ON-based therapeutic, the design should be simple and predictable. Therefore, to make the processes more straightforward, we envisaged making the Zorro in the form of a single-ON entity and we refer to this construct as 'single-stranded Zorro' (ssZorro). In addition, from a size point of view, ssZorro would be smaller than the original 2-ON Zorro. It is well established that small-sized LNA-based therapeutics are more efficient (27,36). A functional ssZorro would therefore presumably also facilitate its formulation and delivery.

In this report, we have developed methods by which we can investigate the binding mechanism of Zorro LNA and its proposed duplex invasion ability. Furthermore, we tested whether the use of ssZorro would affect the DSI efficiency. Finally, we investigated the possibility of exchanging the 7-nt linker in ssZorro by non-nucleotide linkers of different size and hydrophobicity and, moreover, how these modifications would influence both the binding and duplex-invasion properties of the molecule.

MATERIALS AND METHODS

Synthesis of single-stranded Zorro constructs

Mixmer LNA/DNA ON strands (ssZorros) were synthesized by solid phase phosphoramidite chemistry on an automated DNA synthesizer in 1.0 μmol synthesis scale. Standard procedures were used, i.e. trichloroacetic acid in CH_2Cl_2 as the detrytilation reagent, 0.25 M 4,5-dicyanoimidazole (DCI) in CH_3CN as the activator, acetic anhydride in THF as cap A solution, 1-methylimidazole in THF as cap B solution and 0.02 M iodine in H_2O/pyridine/THF as the oxidizing solution. To realize strand polarity reversal, i.e. 3′-5′-5′-3′ syntheses, inverted O3′-DMT O5′-phosphoramidite DNA and LNA amidite building blocks were used together with standard O5′-DMT O3′-phosphoramidite DNA and LNA amidite building blocks. The inverted DNA and standard DNA and LNA amidite building blocks are commercially available whereas the inverted LNA amidite building blocks (5-methyl-C and T derivatives) were synthesized using a recently published procedure (37). For LNA and inverted LNA amidites, extended coupling times (6 min) resulted in stepwise coupling yields of 99%, as obtained for DNA and inverted DNA amidites (2 min coupling time). All ssZorros, except the one having a Cy3 linker element, were prepared with a Cy3 label in the 3′-end of the pyrimidine ssZorro strand. The ssZorro with a 7-nt linker was also synthesized with a Cy5 label for studies involving the Cy3 labeled 'stiffener' ON. The pyrimidine arm was prepared using inverted DNA and LNA amidites after completion of the other Zorro strand and the linker region. Polarity reversal during synthesis was thus implemented after completion of the linker region. For ssZorros containing non-nucleotide linkers, the relevant commercially available linker-building blocks were incorporated using similar amidite chemistry under conditions recommended by the supplier. The TINA (twisted intercalating nucleic acid) linker was synthesized and incorporated into a ssZorro using published procedures (38). The removal of nucleobase-protecting groups and cleavage from solid support was achieved using 32% aq. NH_3 for 24 h at room temperature. Purification to at least 80% purity of all modified ONs was performed by RP-HPLC or IE-HPLC, and the composition of all synthesized ONs was verified by MALDI-MS analysis recorded using 3-hydroxypicolinic acid as a matrix.

LNA/DNA ONs and annealing procedures

Labeled LNA/DNA ONs used for making the conventional 2-ON Zorros were bought from Eurogentec (Belgium). The 'up-ON' was 5′-labeled with a Cy3 dye while the 'down-ON' was 5′-labeled with a Cy5 dye. A 7-base ON complementary to the linker region of

ssZorro, (named 'stiffener') was annealed to the ssZorro to stiffen the linker region (Figure 1a). Stock solutions of the up-ON, down-ON, ssZorro and the stiffener were heated to 95°C for 5 min and then immediately immersed in ice. After cooling, the 2-ON Zorro (20 μM) was formed by mixing the up-ON and the down-ON in an annealing buffer: 10 mM Tris–HCl, pH 7.5, 100 mM NaCl, 1 mM EDTA. Annealing of ssZorro to stiffener followed the same protocol as were control solutions of the up-ON, down-ON, ssZorro and stiffener. All mixtures were heated at 95°C for 10 min followed by slow cooling until reaching room temperature. The annealed constructs were stored at 4°C until used. The annealing was verified using 15% polyacrylamide gels, where bands were visualized using Molecular Imager FX equipment (BioRad, USA) through the Cy3 or Cy5 labels on each ON. A further assessment was done by staining the gels with SYBR® Gold (Invitrogen, Molecular Probes), which mainly stains the dsDNA, as a means to confirm the successful annealing (Figure 1b). LNA/DNA 16-mer ONs representing the up- and down-ONs for Zorro but lacking the linker sequence (Up-16 and Down-16) were also bought from Eurogentec.

Hybridization of plasmid DNA to Zorro constructs

pN25-2BS is a plasmid with two binding sites for the Zorro-LNA previously prepared by standard molecular cloning procedures (33). PN25-0BS, a plasmid lacking Zorro target sites but otherwise with the same sequence as pN25-2BS, was used as control. The final concentration of the plasmid in all hybridization mixes was 0.25 μg/μl (0.1 μM). The plasmid was hybridized with different concentrations of each Zorro construct as well as Up- and Down-16-mer LNA/DNA ONs in concentrations ranging from 0.5 to 8 μM (5–80 times molar excess to plasmid) and the reactions were kept at 37°C for 24 h. Hybridizations were performed in a physiological intracellular buffer with the following composition: 50 mM tris–acetate, 5 mM $MgSO_4$, 100 mM KCl and 10 mM NaCl. Mock treatment was performed by incubating plasmid pN25-2BS with the same buffer under the same conditions but without Zorros. For the kinetics studies, pN25-2BS was hybridized to the different Zorro constructs and linear LNA/DNA ONs at a concentration of 1 or 3 μM using the same conditions as mentioned above. Samples were removed from each reaction after 2, 8, 24, 72 or 144 h for further analyses. PN25-tyr is a plasmid cloned with

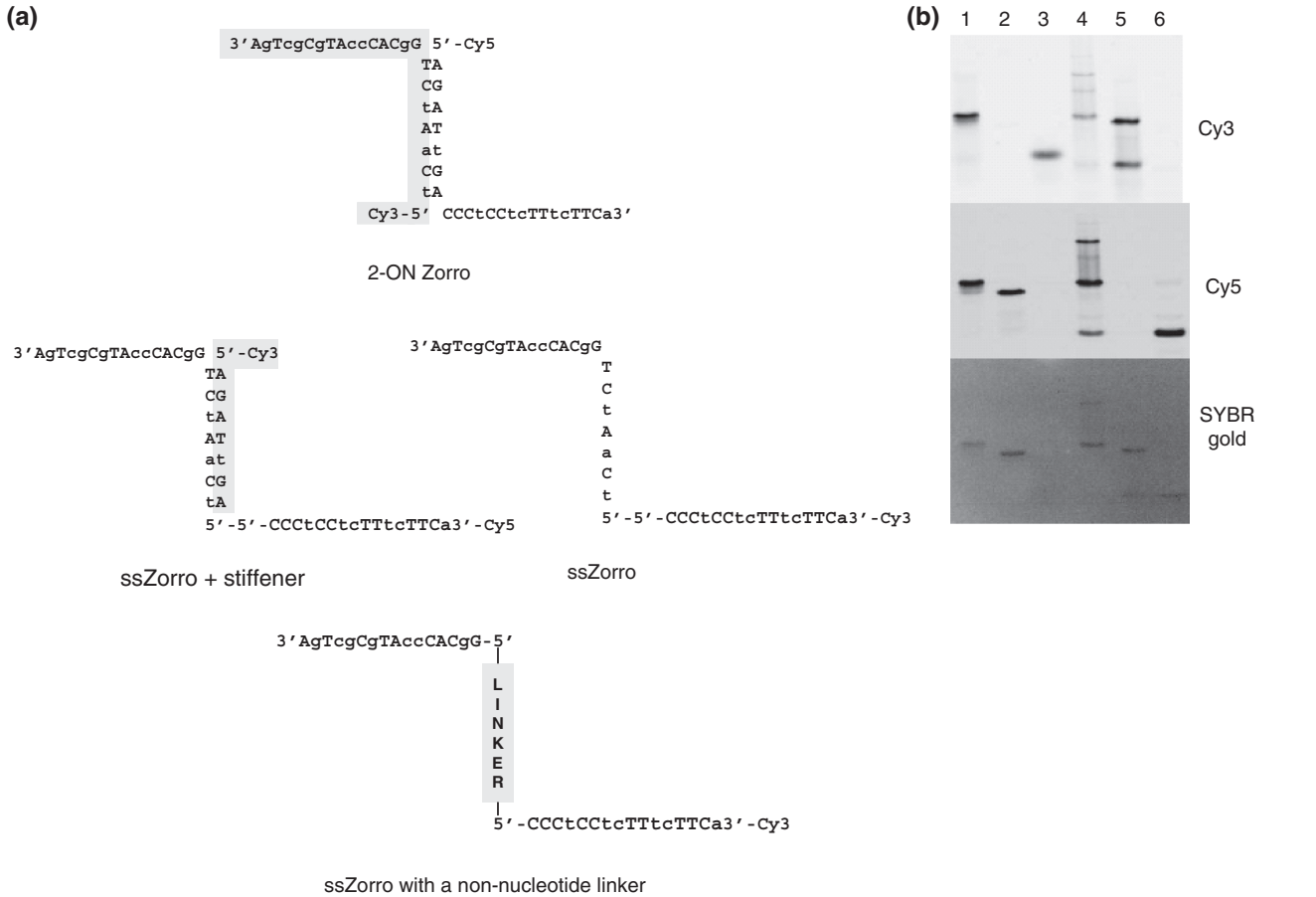

Figure 1. Illustration of Zorro sequences and annealing. (**a**) Schematic representation of 2-ON Zorro, ssZorro linked to the stiffener ON (ssZorro + stiffener), ssZorro and ssZorro with a non-nucleotide based linker. LNA bases are written in capital letters, while DNA bases are in lowercase. (**b**) A 15% polyacrylamide gel showing the annealing of the up- and down-ONs to form the 2-ON Zorro and the annealing of the ssZorro to its stiffener. Lane 1: annealed ssZorro + stiffener, lane 2: ssZorro alone, lane 3: stiffener alone, lane 4: annealed 2-ON Zorro, lane 5: up-ON alone, lane 6: down-ON alone.

two binding sites for a new target sequence derived from the first intron of the tyrosinase (tyr) gene. PN25-tyr was hybridized with the 2-ON Zorro complementary to the new site using the same concentrations and conditions as mentioned above.

Analyzing Zorro binding efficiency by agarose gel electrophoresis

Plasmids hybridized with the different Zorro constructs were analyzed on 0.9 % agarose gels in 1 × Tris-acetate EDTA (TAE) buffer and visualized using Molecular Imager FX equipment through the Cy3 or Cy5 labels on each Zorro construct. For each construct, standards consisting of increasing amounts of Zorro bound to complementary short DNA ONs were loaded on the gel 10 min before the end of the gel run. Using this setting, Zorros bound to short ONs appear at almost the same distance from the wells, thereby optimizing comparative quantification. Standard curves were made from these bands and were used to estimate the amount of Zorro bound to the supercoiled plasmid.

Assessing the double-strand invasion efficiency by S1 nuclease digestion

S1 nuclease is an enzyme that degrades ss DNA. Since the DSI mechanism, proposed for Zorro binding, would lead to the production of ss DNA stretches, it should be possible to measure the DSI efficiency of the different Zorros as increased sensitivity to S1 nuclease in the supercoiled plasmid fraction (Figure 2a). While this enzyme is specific for cutting ss DNA, it might still cause unspecific nicking and degradation of supercoiled ds DNA under non-optimized conditions. Therefore, concentrations and conditions were adjusted to preferentially allow for the specific activity of the enzyme. 0.5 µg of plasmid hybridized with different Zorro constructs or with linear LNA/DNA ONs was digested by 8.3 units of S1 nuclease (Promega, USA) in 1 × S1 nuclease enzyme buffer. The 10 × buffer consists of 500 mM sodium acetate, 2.8 M NaCl and 45 mM $ZnSO_4$ (Promega). The digestion was performed for 4.5 min on ice, and the enzymatic reaction was stopped by adding EDTA to a final concentration of 77 mM. The controls we used were plasmids hybridized with bis-PNA and with a TFO, for sequences see (39) and (40), respectively. Samples from the digestion mixtures were analyzed on 0.9% agarose gels in 1 × TAE buffer and visualized by SYBR® Gold staining. Gels were documented using the Fluor-S system with a cooled CCD camera (BioRad, USA) and analyzed with the Quantity One software (BioRad) (Figure 2b). DSI was calculated by measuring the ratio of supercoiled plasmid in treated preparations, and then dividing the ratios for the hybridized plasmids by the ratio for the mock-treated plasmid after S1 nuclease treatment. For each Zorro construct, we calculated the concentration at which 50% DSI was achieved in the supercoiled plasmid after 24-h incubation at 37°C. The calculated value is referred to as: 'DSI C_{50}'. Similarly, in the kinetics experiments, the time at which 50% DSI occurs at a given Zorro concentration

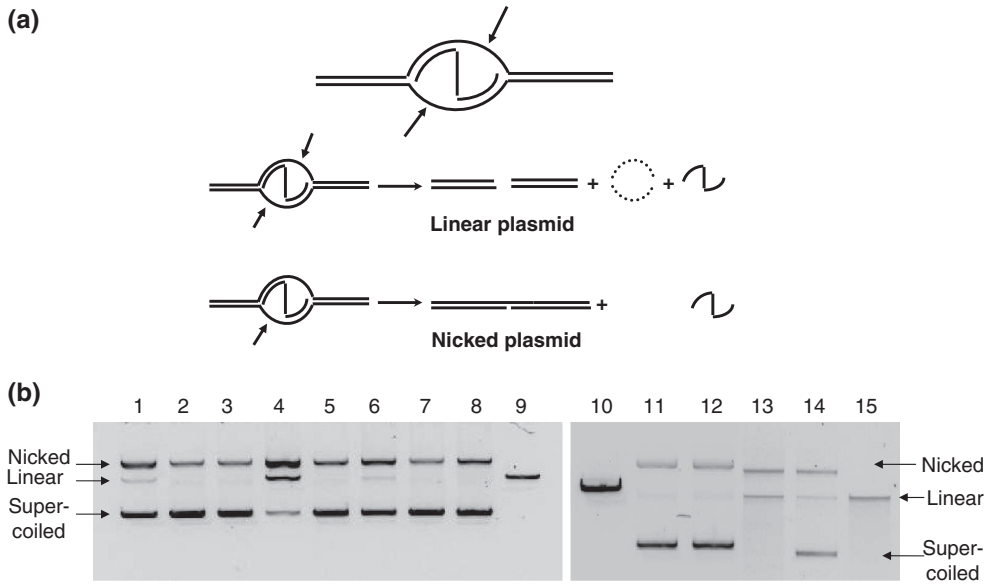

Figure 2. S1 nuclease digestion as a method to demonstrate double-strand invasion of the supercoiled plasmid by Zorro LNA. (**a**) Schematic simplified illustration of how Zorro double-strand invasion will create single-stranded stretches of DNA susceptible to S1 nuclease digestion. As shown by the arrows, the enzyme action will lead to an increase in the nicked plasmid band and/or to a production of the linear form of the plasmid. (**b**) 0.9% agarose gel electrophoresis of plasmids hybridized with different types of ONs and subsequently digested with S1 nuclease. Lanes 1–7 contain pN25-2BS plasmid hybridized with, lane 1: 2-ON Zorro (1 µM), lane 2: up-ON (1 µM), lane 3: down-ON (1 µM), lane 4: 2-ON Zorro (8 µM), lane 5: up-ON (8 µM), lane 6: down-ON (8 µM), lane 7: mock-hybridized pN25-2BS. Lane 8: pN25-0BS hybridized with 2-ON Zorro (8 µM) and lane 9: linear pN25 after digestion with HpaI restriction enzyme. Lanes 11 and 12 contain a plasmid with a TFO binding site hybridized with the corresponding TFO (lane 11) and mock-hybridized (lane 12) both after digestion with S1 nuclease. Lane 10 contains the same plasmid in the linear form. Lanes 13 and 14 contain EGFPLuc-RGB; a plasmid with a bis-PNA binding site hybridized with the corresponding bis-PNA (lane 13) and mock-hybridized (lane 14) both after digestion with S1 nuclease. Lane 15 contains the same plasmid in the linear form.

for each construct is referred to as DSI t_{50}. Thus, DSI C_{50} and DSI t_{50} were used as indicative values for the extent and rate, respectively, of DSI achieved by all Zorro constructs tested in this study.

Statistics

Data are expressed as mean ± standard deviation. Statistical analyses were performed using Student's *t*-test for comparison of means. A probability of less than 0.05 was considered to be statistically significant.

RESULTS

Evidence for invasion of Zorro-LNA into plasmid DNA

Zorro-LNA was designed to function as an anti-gene ON and hypothesized to work through Watson–Crick binding to adjacent sites on both strands of dsDNA (33). The original construct was composed of two ONs hybridized by annealing two complementary 7-nt stretches, which together create the 'linker' region (Figure 1a). In order to study the binding mechanism, the effect of S1 nuclease digestion was investigated. The conditions were optimized to obtain robust digestion of the positive control, bisPNA hybridized to plasmid DNA, without any significant digestion of the negative control, a TFO hybridized to plasmid DNA (Figure 2b). Target plasmid pN25-2BS hybridized with different concentrations of Zorro-LNA showed pronounced digestion by S1 nuclease, while both the mock-treated plasmid and the one devoid of Zorro target sites (pN25-0BS) did not (Figure 2b). A second plasmid, pN25-tyr, hybridized with different concentrations of the corresponding new Zorro showed the same degree of S1 nuclease sensitivity as the hybridized pN25-2BS plasmid (Supplementary Figure S1). These results clearly suggest that Zorro-LNAs indeed are able to strand invade into dsDNA without sequence restrictions.

Development of ssZorro-LNAs and activity assessment

To facilitate the process of designing Zorro sequences for targeting therapeutic genes and to improve cellular uptake, we wanted to combine the two ONs into a single-molecule entity. To allow targeting of both strands of the plasmid with only one ON, the two binding regions should be antiparallel, thus necessitating a 5′-5′ linkage between the two binding arms. The desired 3′-5′-5′-3′ ssZorro (Figure 1a) was prepared by combining 3′- and 5′-phosphoramidites. To investigate whether the use of ssZorro would alter the hybridization and DSI efficiency to plasmid DNA, two assays were used: quantification of fluorescently labeled ssZorro bound to supercoiled plasmids and S1 nuclease digestion. Indeed, we found no reduction in the hybridization efficiency of this new construct (Figure 3a and Supplementary Figure S2). On the contrary, DSI efficiency of ssZorro was significantly higher in both extent and rate than that of the conventional 2-ON Zorro with a DSI C_{50} of 1.2 μM as compared to 3.08 μM (Figure 3b, Supplementary Figure S3 and Table 1). Moreover, kinetics studies demonstrated that ssZorro has a faster rate of DSI into plasmid DNA (DSI t_{50} = 26 and 64 h for 1 μM of ssZorro and 2-ON Zorro, respectively) (Figure 3c and Table 1). Since the original 2-ON Zorro construct contained a rigid ds linker region we also analyzed the DSI efficiency of the ssZorro after annealing the linker to a complementary 7-nt LNA/DNA 'stiffener' (Figure 1a). The DSI of the ssZorro with 'stiffener' was significantly higher than that of the original 2-ON Zorro, although lower than ssZorro LNA alone, both in terms of rate and extent (Figure 3b and c and Table 1).

Evaluating the DSI capacity of short linear LNA/DNA ONs

In order to evaluate whether short LNA/DNA mixmer ONs can strand invade duplex DNA, we tested the two 16-mer LNA/DNA ONs, Up-16 and Down-16, for strand invasion. The Up-16 failed to strand invade plasmid DNA even at the highest concentration tested. The Down-16 could, on the contrary, achieve DSI even at very low concentrations and at a fast rate, significantly different from the ssZorro construct (DSI C_{50} = 0.6 μM and DSI t_{50} = 8 h) (Figure 4). However, comparing the S1 nuclease assays for Down-16 and for ssZorro, it is clear that the invasion by the short ON leads mainly to an increase in the nicking of the plasmid while the invasion by Zorros results in a higher proportion of linearized plasmid DNA as well as a higher total nuclease sensitivity (nicked + linearized plasmid) (Figure 4b, c and d). Interestingly, when performing hybridization of the plasmid with the up-ON and with the down-ON (same sequences as for Up-16 and Down-16 but with an extension consisting of the 7-bases linker part), neither of these ONs showed any sign of DSI (Figure 2b: lanes 2, 3, 5 and 6 and Figure 4c). These facts exclude the possibility that Zorro-LNA is hybridizing only through binding of its lower arm.

Effect of linker modifications on the activity of ssZorro-LNA

Subsequently, we synthesized ssZorros with linkers based on non-nucleotide chemistries (Figure 5). These linkers were of variable size and hydrophobicity. First we tested two PEG-based linkers of different length: a triethylene glycol phosphate: (TEG) and a di (hexaethylene glycol phosphate): (HEG × 2) linker. The TEG linker construct showed similar hybridization efficiency as that of the original ssZorro while the DSI decreased significantly with a DSI C_{50} of 2 μM and a DSI t_{50} of 46 h (Figure 6b and c and Table 1). Conversely, the longer HEG × 2 displayed a marked increase in the hybridization that even exceeded 100% at concentrations higher than 1 μM (Figure 6a and Supplementary Figure S2). However, this construct behaved similar to the original ssZorro in the S1 nuclease assay (Figure 6b and c, Supplementary Figure S3 and Table 1). Both the constructs with PEG-based linkers reached a significantly higher DSI than that of the 7-nt linker construct after 144-h incubation at 3 μM (Figure 6d).

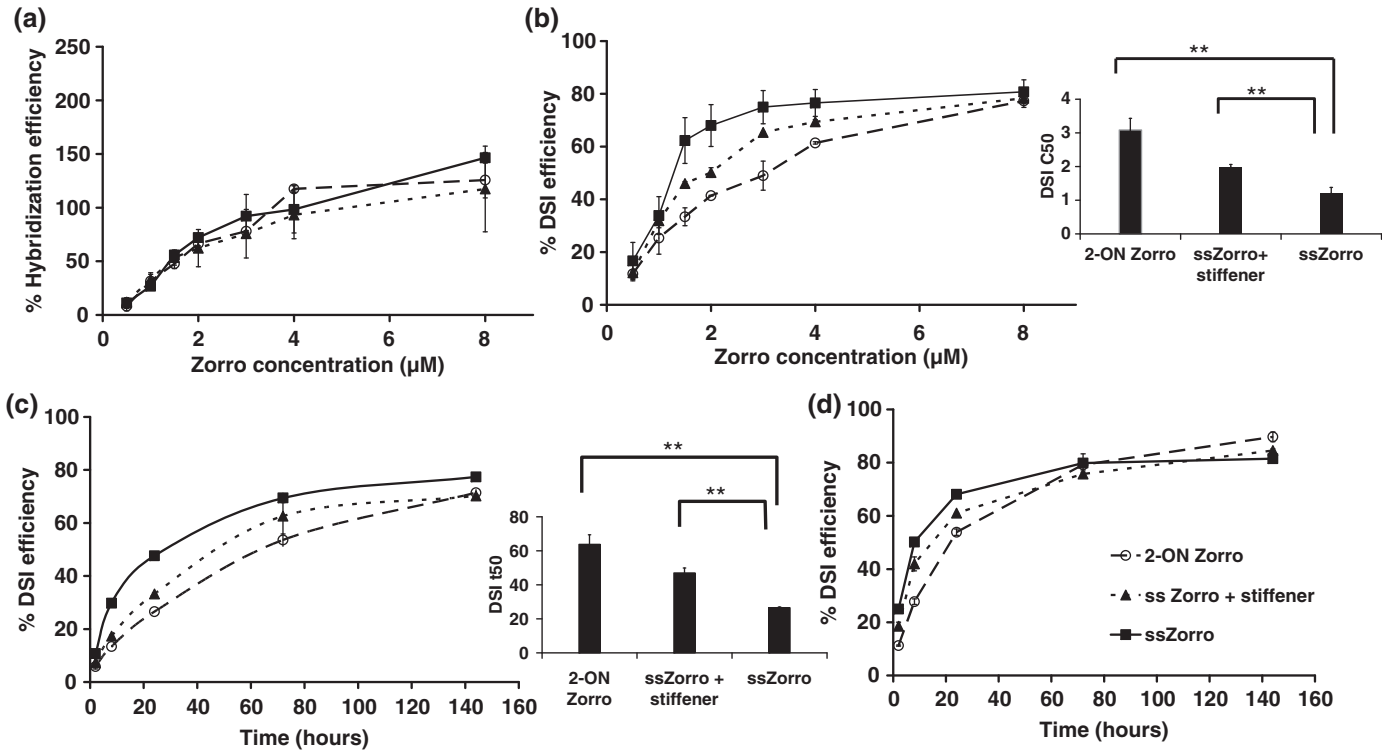

Figure 3. Hybridization and double-strand invasion (DSI) efficiency of 2-ON Zorro, ssZorro and ssZorro + stiffener. (**a**) Hybridization efficiency of the three Zorro constructs at concentrations ranging from 0.5 to 8 μM. PN25-2BS was incubated with the different constructs at 37°C for 24 h in the physiological buffer with intracellular ion concentration. (**b**) DSI efficiency of the three Zorro constructs at the same concentrations as in A. After 24-h incubation time, 0.5 μg of each reaction was treated with S1 nuclease as described in the 'Materials and methods' section. Differences in the DSI C_{50} by ssZorro, ssZorro + stiffener and 2-ON Zorro were significant (**$P < 0.01$). (**c**) Kinetics of the DSI elicited by the Zorro constructs at a concentration of 1 μM. Differences in DSI t_{50} by ssZorro, ssZorro + stiffener and the 2-ON Zorro were significant (**$P < 0.01$). (**d**) Kinetics of the DSI produced by the Zorro constructs at 3 μM concentration.

Table 1. Values of DSI C_{50} and DSI t_{50} of the different Zorro constructs used

Construct	DSI C_{50} (μM)	DSI t_{50} (h)
2-ON Zorro	3.09 (0.35)**	63.8 (5.0)**
ssZorro + stiffener	1.99 (0.071)**	47.0 (2.9)**
ssZorro	1.21 (0.17)	26.5 (0.5)

ssZorro with different linkers

Linker	The number of atoms between the two 5′-O	DSI C_{50} in μM	DSI t_{50} in hrs
7 nt	41	1.21 (0.17)	26.5 (0.5)
TEG	12	1.93 (0.01)*	46.1 (3.6)***
HEG × 2	41	1.36 (0)	32.7 (5.4)
C3	7	1.49 (0.14)	48.9 (2.9)***
C12	16	1.79 (0.048)	81.3 (1.8)*
C12 × 3	46	7.15 (0.83)***	>144
Linker-less	1	1.63 (0.11)*	45.4 (1.2)***
Cy3	15	2.92 (0.12)**	97.0 (12.1)****
TINA	6	3.59 (0.17)***	>144
Linker-less with glycylamino LNA-T	1	1.48 (0.07)	42.6 (0.6)

All comparisons were made to the ssZorro with the 7-nt linker and significance is represented in stars. The number of atoms connecting the two 5′ oxygens is also shown for each ssZorro construct.

We further tested a series of alkyl-chains of 3 (propyl), 12 (dodecyl) and 36 (tri-dodecyl) atoms' length as hydrophobic linkers for the ssZorro LNA (Figure 5). These linkers clearly influenced Zorro hybridization to plasmid DNA in different ways. The C3 linker behaved similar to the 7-nt ssZorro, while the longest one (C12 × 3) displayed the lowest hybridization efficiency of all linkers tested in the study. The intermediate C12 linker showed an increase in hybridization similar to that observed for the HEG × 2 linker; however, >100% hybridization at concentrations higher than 2 μM is also generated (Figure 7a and Supplementary Figure S2). Regarding the strand invasion, incorporation of the C12 × 3 linker, being similar in size as the hydrophilic HEG × 2 linker (Table 1), resulted in a drastic decrease in DSI efficiency. It showed the highest DSI C_{50} value of all constructs (7.1 μM) and the DSI t_{50} exceeded our endpoint of 144 h (Figure 7b and c, Supplementary Figure S3 and Table 1). On the other hand, the constructs with the shorter hydrophobic linkers (C3 and C12) showed a similar efficiency in DSI as that with the original 7-nt linker ssZorro (Figure 7b and Supplementary Figure S3). After 144 h at 3 μM concentration the C12 construct even displayed a significantly higher plateau value than that of the original ssZorro (Figure 7d). Notably, both the C3 and C12 constructs strand invaded at a significantly slower

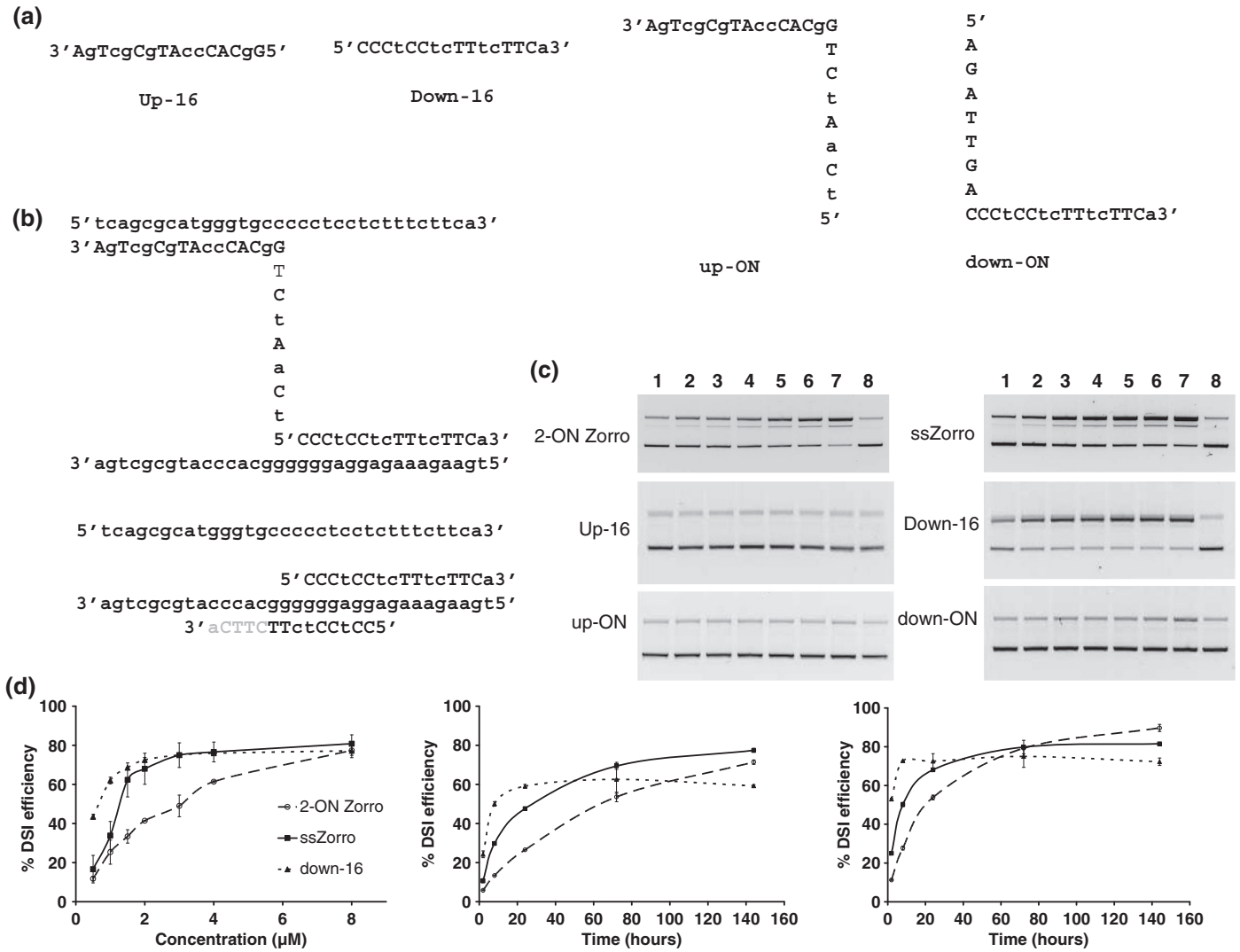

Figure 4. Evaluation of short LNA/DNA ONs for double-strand invasion (DSI) into plasmid DNA. (**a**) Sequences of the ss LNA/DNA ONs tested for DSI: Up-16, Down-16, up-ON and down-ON. (**b**) Upper and lower panels: illustrations of the predicted base pairing of ssZorro and the ON designated Down-16 to ds DNA, respectively. The representation of the Down-16 binding shows the stretch of the ON with capacity to bind as a TFO by Hoogsteen base pairing in black while the rest of the ON is in gray. (**c**) Agarose gels showing the DSI achieved by 2-ON Zorro, ssZorro and the corresponding ss LNA/DNA ONs after S1 nuclease digestion. Order of lanes in each gel from 1 to 7 is as follows: plasmid hybridized with 0.5, 1 and 1.5, 2, 3, 4, 8 μM of the respective ON. Lane 8 is the mock-treated plasmid. (**d**) The left graph shows quantification of the DSI of Down-16 compared to that of ssZorro and 2-ON Zorro at different concentrations. The middle graph represents the kinetics of the three constructs at 1 μM while the graph to the right shows kinetics at 3 μM.

rate than the 7-nt linker construct at 1 μM (Figure 7c and Table 1).

We also tested additional linkers having other properties. Thus, as one extreme, we synthesized a linker-less ssZorro with just a phosphate group (i.e only one atom connecting the two arms), one construct with the well-known Cy3 dye as a rigid linker and finally an ssZorro with a TINA (38,40) monomer linker (Figure 5). Both the linker-less ssZorro and the ssZorro with Cy3 linker resulted in similar hybridization efficiency as the parent ssZorro (Figure 8a and Supplementary Figure S2). However, both constructs showed significantly higher DSI C_{50} and t_{50} values compared to the 7-nt linker construct (Figure 8b and c, Supplementary Figure S3 and Table 1). Still the linker-less construct reached the same total DSI as the original ssZorro within 144 h at 1 μM concentration, while the Cy3-linker did not (Figure 8c). Finally, the ssZorro with the intercalating base, TINA, also displayed similar hybridization efficiency although the hybridization exceeded 100% at higher concentrations (≥4 μM) (Figure 8a). Conversely, this linker significantly decreased the total DSI as well as the DSI rate, yielding a DSI C_{50} value of 3.6 μM and a DSI t_{50} value greater than 144 h (Figure 8b and c and Table 1).

Altogether, linkers of high or medium hydrophobicity were found to be optimal for double-strand invasion. The extent of the DSI for the shortest alkyl-chain linker (C3) was similar, while the rate was significantly slower as compared to the ssZorro with the 7-nt linker. The PEG-based linkers and the dodecyl hydrophobic linker

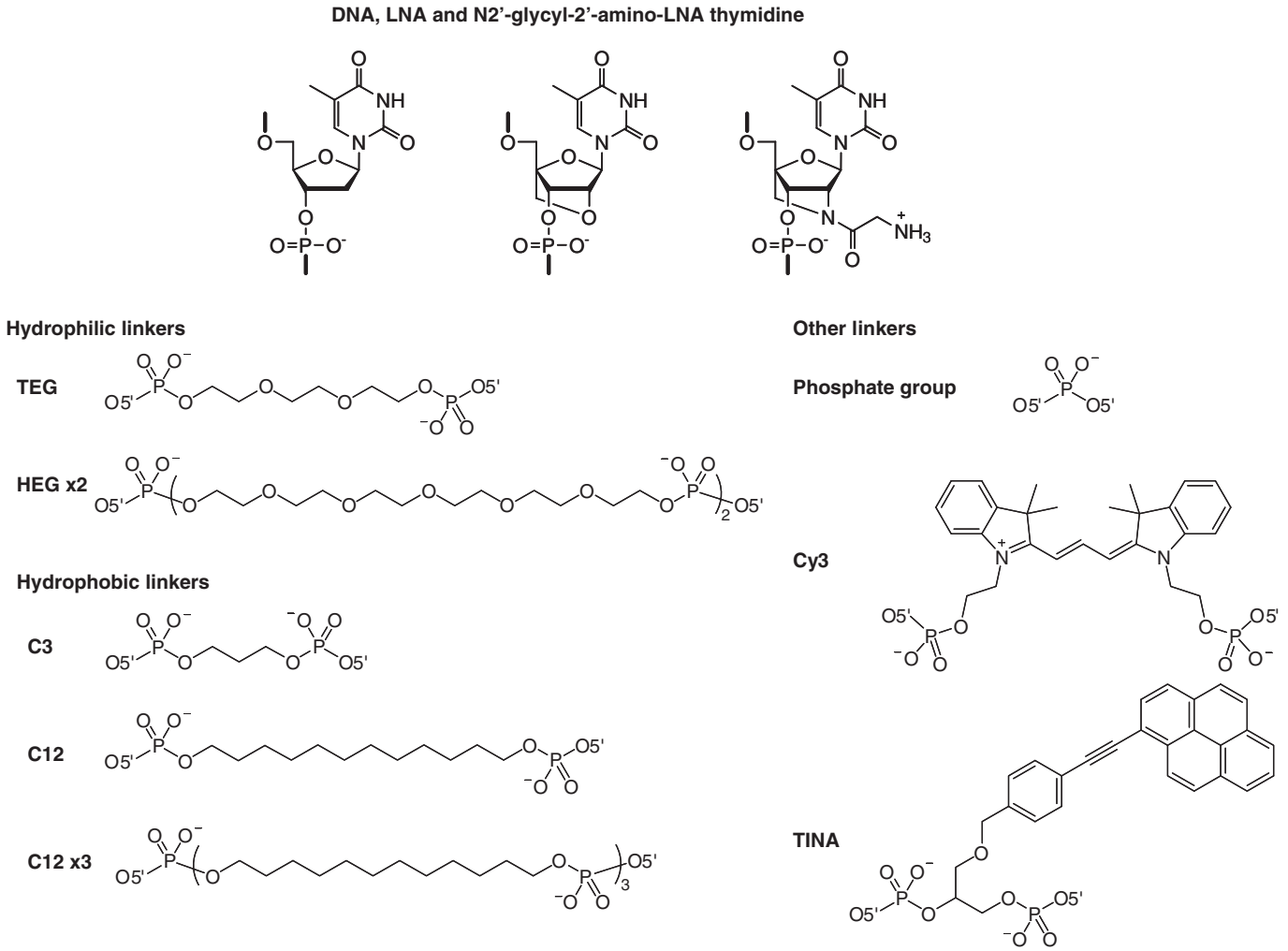

Figure 5. At the top, illustrations of the different types of nucleic acids used in the study, from left to right: DNA, LNA and N2′-glycyl-2′-amino-LNA thymidine. At the bottom, illustrations of the chemical structures of the different linkers used in the study.

(C12) both reached a saturation level significantly higher than that of the 7-nt linker (Figures 6d and 7d). These differences were clearly demonstrable at lower concentrations. At 3 μM, the discrimination was less visible, since all other linkers applied in the study reached the same saturation level as that of the 7-nt construct, except for the longest hydrophobic one (C12 × 3), which did not even reach the plateau value (Figure 7d).

Effect of LNA modifications in the upper arm on binding and DSI efficiency

Incorporation of N2′-glycyl modified 2′-amino-LNA (Figure 5) into the TFO has been shown to increase thermal affinity of triplexes, presumably due to the positive charge introduced by the protonated amino group of the pendant glycyl moiety (41). Therefore, we tested if the introduction of this modification in ssZorro would enhance its hybridization and DSI efficiency. A linker-less ssZorro LNA containing two N2′-glycyl-2′-amino-LNA thymidine (glycylamino LNA-T) monomers in the upper arm was synthesized. As demonstrated in Supplementary Figure S4a, at concentrations of 2 μM or higher, the glycylamino LNA-T-modified ssZorro elicited a high degree of hybridization, even exceeding 100%. This implies the involvement of altered binding of the modified ssZorro as compared to the native construct. However, the DSI efficiency was not significantly different for the glycylamino LNA-T when compared to the corresponding construct without this modification (Supplementary Figures S3, S4b, S4c and Table 1). Interestingly, looking at the kinetics data, there is a slightly increased rate of DSI at 24 h (Supplementary Figure S4c). This difference was small but significant, suggesting that such modification could be advantageous and should be further investigated.

DISCUSSION

In this study, we conclusively demonstrated that an LNA-based oligonucleotide can strand invade into duplex DNA. Even though the structural nature of Zorro and previous results strongly indicated that the LNA binding to duplex DNA predominantly occurs through strand invasion, this was earlier not formally

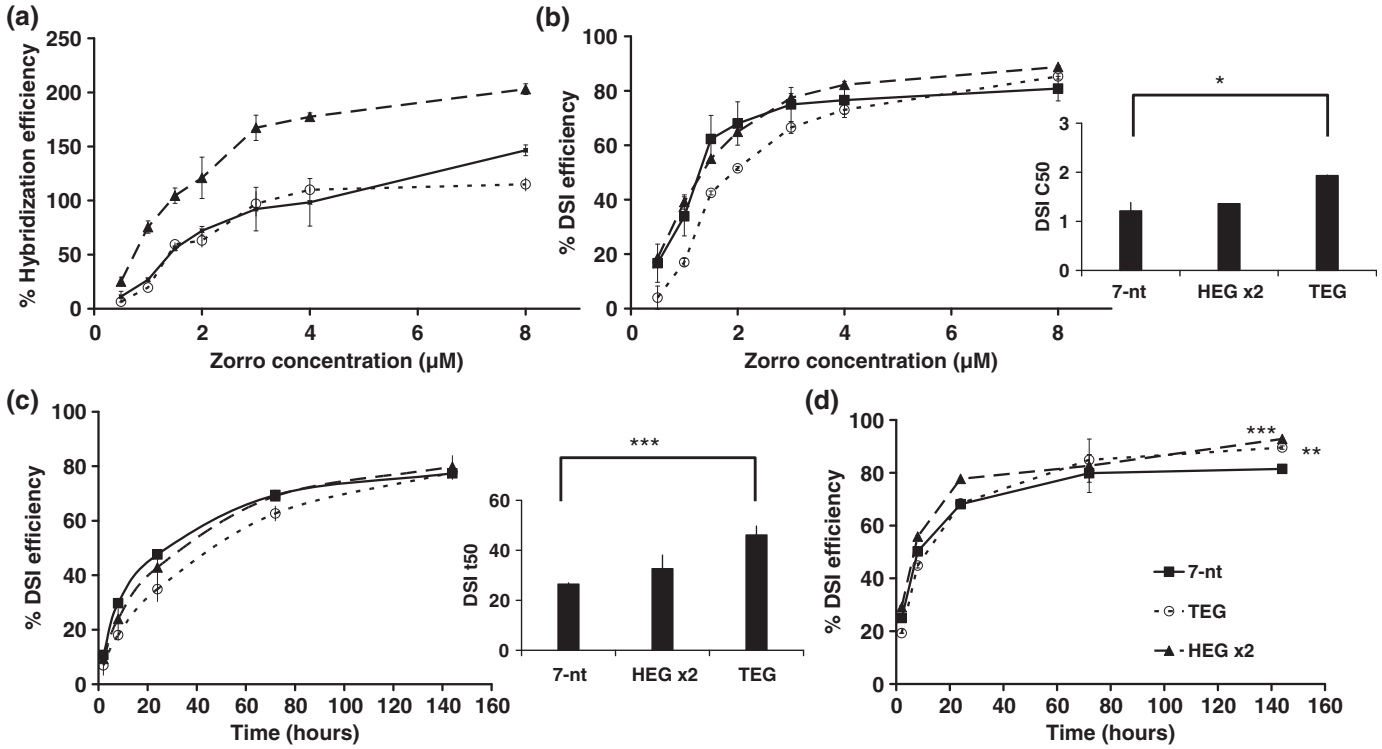

Figure 6. Hybridization and double-strand invasion (DSI) efficiency of ssZorro constructs with hydrophilic PEG linkers. SsZorro constructs with a triethylene glycol phosphate (TEG) and a di (hexaethylene glycol phosphate) (HEG ×2) linker were used and compared to the construct with the 7-nt linker. (**a**) Hybridization efficiency of the three ssZorro constructs at concentrations ranging from 0.5 to 8 μM. PN25-2BS was incubated with the different constructs at 37°C for 24 h in the physiological buffer with an intracellular ion concentration. (**b**) DSI efficiency of the ssZorro constructs at the same concentrations as in A. After 24-h incubation time, 0.5 μg of each reaction was treated with S1 nuclease as described in the 'Methods' section. The difference in the DSI C_{50} elicited by ss Zorros with the 7-nt linker and with the TEG linker was significant ($*P < 0.05$). (**c**) Kinetics of the DSI produced by the ssZorro constructs at a concentration of 1 μM. The difference in DSI t_{50} elicited by ssZorros with the 7 nt and the TEG linker was significant ($***P < 0.001$). (**d**) Kinetics of the DSI produced by the ssZorro constructs at 3 μM. DSI of the TEG and the HEG ×2 linker constructs were significantly higher than that elicited by the 7-nt linker at 144 h ($**P < 0.01$, $***P < 0.001$), respectively.

proven (33,35,42). Since DSI causes the production of ss stretches in DNA, we made use of S1 nuclease digestion as a method to investigate if DSI is the main mechanism for Zorro LNA hybridization. Demidov *et al.* used S1 nuclease digestion for proving strand invasion of PNA (43). However, they carried out this assay on a linearized plasmid. In contrast, when Zelphati *et al.* used S1 nuclease to investigate the DSI properties of PNA for supercoiled plasmid DNA, they obtained the same sensitivity to the enzyme with and without PNA, i.e both forms showed great degree of digestion by the enzyme (44). Presumably, this can be attributed to the unspecific effect of this vigorous enzyme, which, due to the breathing of the supercoiled DNA, can easily digest plasmid DNA under non-optimal conditions. Here, we managed to successfully optimize concentration and other conditions to preferentially detect the specific action of S1 nuclease. In our hands, to get a clear double-strand invasion, we needed the specific design of Zorro LNA, since ssLNA ONs with the extension (up-ON, down-ON) binding to only one of the strands of the duplex did not show any evidence of DSI (Figure 2b and Supplementary Figure S3). Interestingly when testing the shorter LNA/DNA 16-mers (without extension), we found that one of the two ONs (Down-16) could also perform DSI. The possible reason can be that a part of the Down-16 ON (a stretch of 9 bases) can bind as a TFO, facilitating the invasion of the whole ON and the binding via Watson–Crick mode, a mechanism already proposed for bisPNA binding (45). When analyzing the gels for DSI (Figure 4c), we observe that the reduction in the supercoiled plasmid is extremely prominent even at low concentrations. However, the S1 nuclease only cuts in one strand leading to a high increase in nicked plasmid. Oppositely, after Zorro-LNA mediated DSI, the nuclease treatment resulted both in increased nicking and linearization of the supercoiled plasmid, indicating a different mode of invasion performed by Zorros, which affects both DNA strands. The Up-16 did not show any sign of invasion indicating a sequence restriction for strand invasion of short linear LNA/DNA ONs. In this report we also verified the DSI capacity of a second Zorro directed against a new target site devoid of the TFO sequence. This strongly confirms the versatility of Zorros to strand invade without any sequence restrictions. While the ssZorro used in this study targets a site located in the 5′ transcribed, but untranslated region (5′-UTR), the linear LNA used by Corey and coworkers overlap the actual transcription start site (31,35). It will be interesting to investigate the possible targets and to carefully compare

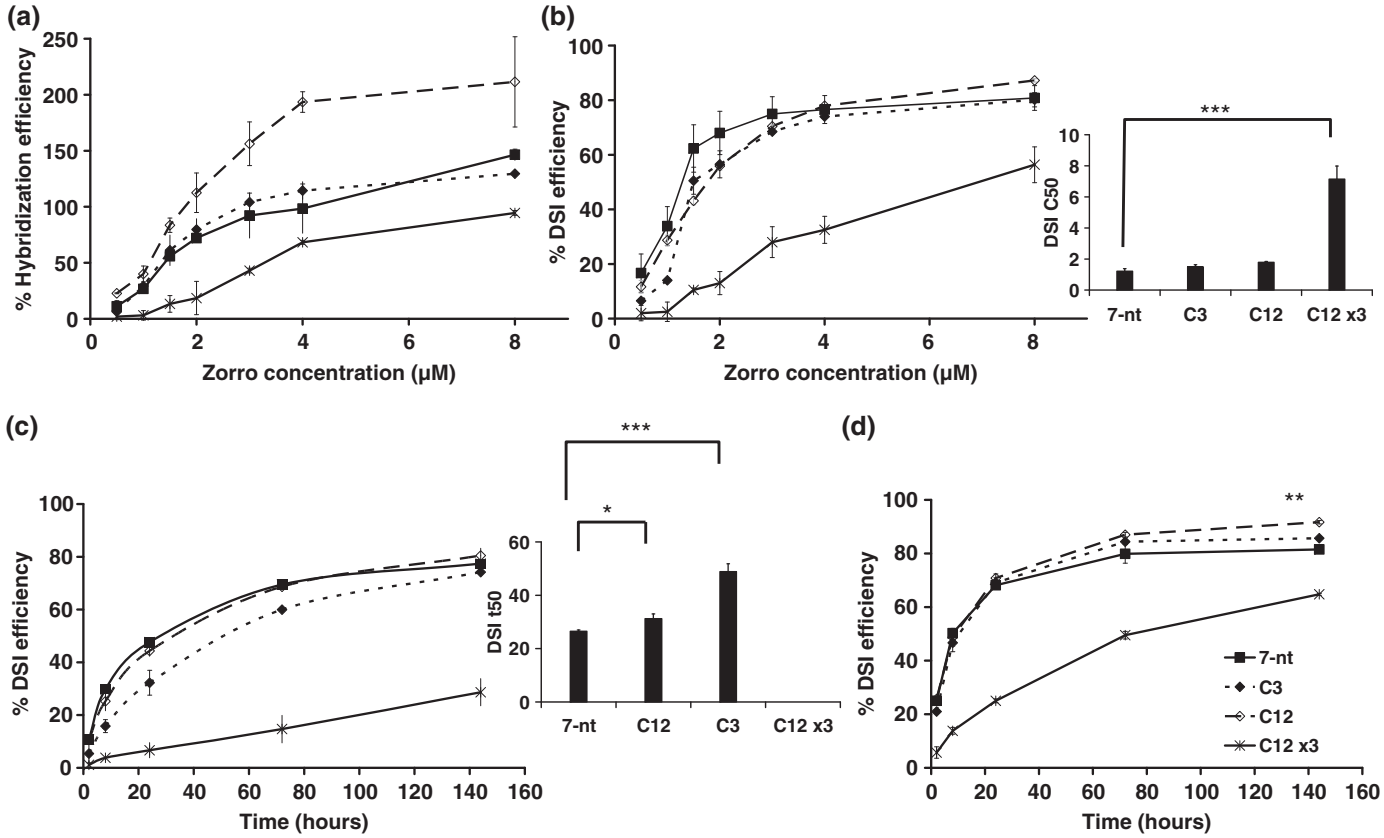

Figure 7. Hybridization and double-strand invasion (DSI) efficiency of the ssZorro constructs with alkyl-chain linkers. SsZorro with the linkers: propyl (C3), dodecyl (C12) and tridodecyl (C12 ×3) were used and compared to the construct with the 7-nt linker. (**a**) Hybridization efficiency of the ssZorro constructs at concentrations ranging from 0.5 to 8 μM. PN25-2BS was incubated with the different constructs at 37°C for 24 h in the physiological buffer with intracellular ion concentration. (**b**) DSI efficiency of the ssZorro constructs at the same concentrations as in (a). After 24-h incubation time, 0.5 μg of each reaction was treated with S1 nuclease. Differences in the DSI C_{50} showed by ssZorros with the 7-nt linker and with the C12 ×3 linker was significant (***$P < 0.001$). (**c**) Kinetics of the DSI elicited by the ssZorro constructs at a concentration of 1 μM. Differences in DSI t_{50} elicited by ssZorro with the 7-base linker and those by ssZorro with the C3 and C12 linkers were significant (***$P < 0.001$) and (*$P < 0.05$), respectively. DSI t_{50} for the construct with the C12 ×3 linker could not be determined (>144 h). (**d**) Kinetics of the DSI elicited by the ssZorro constructs at 3 μM concentration. The construct with the C12 linker achieved a significantly higher DSI than that of the 7-nt ssZorro at 144 h (**$P < 0.01$).

the influence of a number of different locations (promoter, 5′ and 3′ untranslated regions, coding and intronic regions) to identify optimal Zorro target sites *in vivo*.

Agarose gel electrophoresis is a method that has been frequently used to study the binding of labeled ONs to plasmid DNA (39,44,46). With this method, we could determine the hybridization efficiency to the supercoiled plasmid DNA; however, it was not possible to deduce the mechanism by which binding occurs. Interestingly, using our method of estimation, >100% binding was observed for 4 of 12 constructs, suggesting alternative binding modes. One possibility would be that two Zorros would bind to the same target site, where the up-arm of one Zorro binds to one strand of the duplex, while the down-arm of another Zorro binds the opposite strand. This was addressed by making short DNA ONs complementary to the resulting free Zorro arms. Only very low levels of binding were observed (data not shown), arguing against such an explanation. This observation is also of general interest, since it strengthens the hypothesized model for Zorro binding, where a single Zorro simultaneously binds both strands in a Watson–Crick mode. Another alternative would be TFO-binding. Owing to that one of the Zorro arms contains a polypyrimidine stretch, it is possible that such binding could occur. However, we cannot explain why only some of our constructs would demonstrate this form of interaction. Thus, at present we cannot conclusively explain the enhanced binding observed for some of the constructs at high concentrations. Since our main objective in this paper was to investigate DSI as a mechanism for binding of LNA in the form of Zorro, we focused on developing the methods for this purpose.

Since the DSI of ssZorro was higher than that of the original design with a ds linker region, we went on to further optimize this specific construct. Indeed, the new design of Zorro LNA has several advantages. It allows for the use of short linkers or even linker-less constructs, which will further reduce the molecular weight. It also makes the synthesis easier. Owing to the strong binding of LNA to DNA, internal hybridization could occur between the bases in the arm and linker regions during

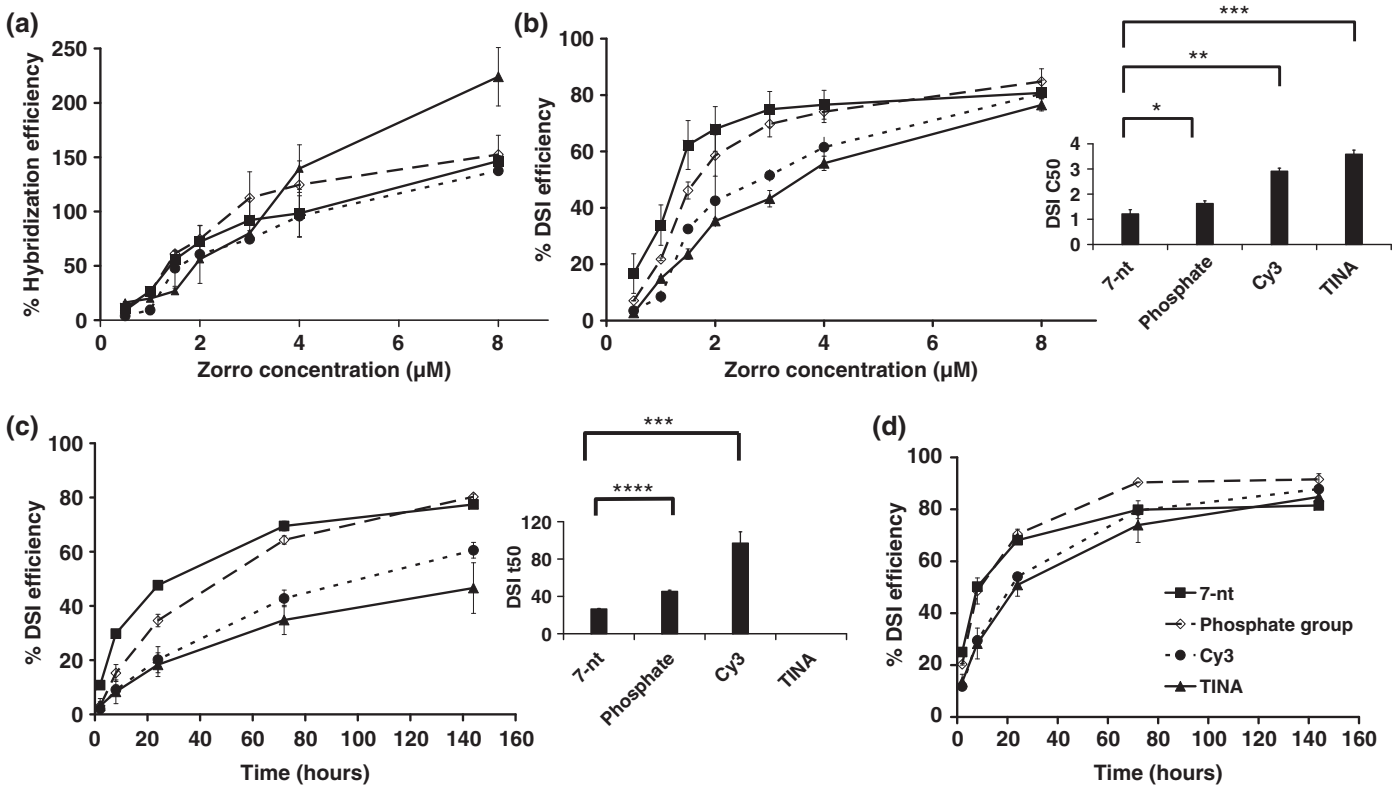

Figure 8. Hybridization and double-strand invasion (DSI) efficiency of the ssZorro constructs with a Cy3-linker, a TINA-linker or with a phosphate group (phosphate) linker (linker-less construct) compared to the construct with the 7-nt linker. (**a**) Hybridization efficiency of the ssZorro constructs at concentrations ranging from 0.5 to 8 μM. PN25-2BS was incubated with the different constructs at 37°C for 24 h in a physiological buffer with an intracellular ion concentration. (**b**) DSI efficiency of the four ssZorro constructs at the same concentrations as in (a). After 24-h incubation time, 0.5 μg of each reaction was treated with S1 nuclease. Differences in the DSI C_{50} elicited by ssZorros with the 7-nt linker and with the Cy3 or TINA linkers as well as the linker-less construct were significant (**$P < 0.01$), (***$P < 0.001$), (****$P < 0.0001$) and (*$P < 0.05$), respectively. (**c**) Kinetics of the DSI produced by the ssZorro constructs at a concentration of 1 μM. Differences in DSI t_{50} elicited by ssZorros with the 7-nt and the Cy3 linkers as well as the linker-less construct were significant (***$P < 0.01$). DSI t_{50} for the construct with the TINA linker could not be determined (>144 h). (**d**) Kinetics of the DSI elicited by the ssZorro constructs at 3 μM concentration.

the annealing phase. This problem is reduced with the design of ssZorros and could be obviated by using non-nucleotide-based linkers. Thus, in the series of constructs that we tested, we first modified the linker region, making it non-nucleotide based. Application of non-nucleotide linkers has been previously investigated in many ON-based approaches such as ribozymes and circular ONs (47,48). Furthermore, bioconjugation of ONs with polymers is widely used for improving penetration and for the purpose of stability (49,50). For instance, conjugation with PEG of different chain length has been addressed in many reports for ONs of DNA, LNA and PNA bases (51–53). From our results, it seems that the flexibility of the linker is playing an important role in obtaining high degrees of double-strand invasion by the ssZorro. Both PEG-based linkers used in the study and the alkyl-chain linker with intermediate length showed prominent DSI. However, the longest alkyl-chain linker (C12 × 3), although having the highest degree of flexibility, showed very poor DSI ability. This could be explained by the hydrophobicity, which could increase aggregation, thereby making this construct less available for strand invasion. When a TINA monomer was used as a linker, it decreased both the rate and the extent of the DSI, which presumably could be explained by the intercalating nature of this linker. Since we believe that the smaller the size of the ssZorro, the more feasible will be its formulation and delivery, we also investigated the use of the linker-less construct. Although this construct displayed reduced DSI C_{50} and t_{50} values, it eventually reached a high plateau level of DSI, similar to that of the ssZorro with the 7-nt linker. This shows that strand invasion of ds DNA can be achieved, using the smallest (32 nt in length) of all tested Zorros.

Importantly, Zorro LNAs were found not to block replication, which may be of importance from a safety point of view (33). For this reason we anticipate that resting, or slowly dividing, cells may be the best targets for Zorro LNAs. The fact that strand invasion is rather slow (the lowest DSI t_{50} was 26 h) would likely pose a problem when targeting genes in rapidly dividing cells *in vivo*, while for resting, or slowly dividing, cells this may not be the case. Still, we wanted to investigate whether modifications of the LNA bases themselves could further enhance DSI. This was attempted by including LNA-bases containing glycylamino LNA, instead of regular LNA, in one of the arms of ssZorro. As compared to the most well-known synthetic ON with DSI capability,

namely PNA, native LNA is negatively charged and this is likely to impair DSI. Introduction of positive charges reduces the overall charge of the ON, thereby potentially improving DSI ability. Moreover, molecules with targeting capabilities such as certain lipids and peptides can be attached to the glycyl group for further improving the delivery and activity of the ssZorro. Currently, owing to the fact that glycyl phosphoroamidites so far only exist for thymine bases and that for technical reasons the lower arm could not be modified, only 2 of the 32 nt were glycylamino LNA. Even so, from our results it seems as if this had a slight beneficial effect, suggesting that additional modifications further reducing the negative charge could have significant impact on DSI. This is very encouraging and implicates that a careful design of the ON combined with the selection of building blocks with special properties is a key for the development of ONs with enhanced activity. Given the fact that the chemical universe is vast and that the development of synthetic ON analogues has barely come of age, this bodes well for future pharmaceutical approaches.

SUPPLEMENTARY DATA

Supplementary Data are available at NAR Online.

FUNDING

European Union Grant (FP-037283); Arosenius Foundation, the Egyptian Ministry of Higher Education (to E.M.Z.); Danish National Research Foundation (to J.W.); Swedish Research Council and the Torsten and Ragnar Söderberg Foundation. Funding for open access charge: Swedish Research Council.

Conflict of interest statement. None declared.

REFERENCES

1. Harper,S.Q. (2009) Progress and challenges in RNA interference therapy for Huntington disease. *Arch. Neurol.*, **66**, 933–938.
2. Sahu,N.K., Shilakari,G., Nayak,A. and Kohli,D.V. (2007) Antisense technology: a selective tool for gene expression regulation and gene targeting. *Curr. Pharm. Biotechnol.*, **8**, 291–304.
3. Uil,T.G., Haisma,H.J. and Rots,M.G. (2003) Therapeutic modulation of endogenous gene function by agents with designed DNA-sequence specificities. *Nucleic Acids Res.*, **31**, 6064–6078.
4. Ashihara,E., Kawata,E. and Maekawa,T. (2009) Future prospect of RNA interference for cancer therapies. *Curr. Drug Targets*, **11**, 345–360.
5. Bennett,C.F. and Swayze,E.E. (2010) RNA targeting therapeutics: molecular mechanisms of antisense oligonucleotides as a therapeutic platform. *Annu. Rev. Pharmacol. Toxicol.*, **50**, 259–293.
6. Wood,M.J., Gait,M.J. and Yin,H. (2010) RNA-targeted splice-correction therapy for neuromuscular disease. *Brain*, **133**, 957–972.
7. Young,D.D., Lively,M.O. and Deiters,A. (2010) Activation and deactivation of DNAzyme and antisense function with light for the photochemical regulation of gene expression in mammalian cells. *J. Am. Chem. Soc.*, **132**, 6183–6193.
8. Hall,P.A., Reis-Filho,J.S., Tomlinson,I.P. and Poulsom,R. (2010) An introduction to genes, genomes and disease. *J. Pathol.*, **220**, 109–113.
9. Lundin,K.E., Simonson,O.E., Moreno,P.M., Zaghloul,E.M., Oprea,II., Svahn,M.G. and Smith,C.I. (2009) Nanotechnology approaches for gene transfer. *Genetica*, **137**, 47–56.
10. Hansen,M.E., Bentin,T. and Nielsen,P.E. (2009) High-affinity triplex targeting of double stranded DNA using chemically modified peptide nucleic acid oligomers. *Nucleic Acids Res.*, **37**, 4498–4507.
11. Besch,R., Giovannangeli,C. and Degitz,K. (2004) Triplex-forming oligonucleotides - sequence-specific DNA ligands as tools for gene inhibition and for modulation of DNA-associated functions. *Curr. Drug Targets*, **5**, 691–703.
12. Wu,Q., Gaddis,S.S., MacLeod,M.C., Walborg,E.F., Thames,H.D., DiGiovanni,J. and Vasquez,K.M. (2007) High-affinity triplex-forming oligonucleotide target sequences in mammalian genomes. *Mol. Carcinog.*, **46**, 15–23.
13. Bentin,T., Hansen,G.I. and Nielsen,P.E. (2006) Structural diversity of target-specific homopyrimidine peptide nucleic acid-dsDNA complexes. *Nucleic Acids Res.*, **34**, 5790–5799.
14. Vekhoff,P., Ceccaldi,A., Polverari,D., Pylouster,J., Pisano,C. and Arimondo,P.B. (2008) Triplex formation on DNA targets: how to choose the oligonucleotide. *Biochemistry*, **47**, 12277–12289.
15. Boutorine,A.S., Doluca,O. and Filichev,V.V. (2009) Optimization of the sequence of twisted intercalating nucleic acids (TINA) forming triple helix with the polypurine tract of the proviral HIV DNA, *Nucleic Acids Symp. Ser. (Oxford)*, 139–140.
16. Gaddis,S.S., Wu,Q., Thames,H.D., DiGiovanni,J., Walborg,E.F., MacLeod,M.C. and Vasquez,K.M. (2006) A web-based search engine for triplex-forming oligonucleotide target sequences. *Oligonucleotides*, **16**, 196–201.
17. Vasquez,K.M., Christensen,J., Li,L., Finch,R.A. and Glazer,P.M. (2002) Human XPA and RPA DNA repair proteins participate in specific recognition of triplex-induced helical distortions. *Proc. Natl Acad. Sci. U S A*, **99**, 5848–5853.
18. Bomholt,N., Osman,A.M. and Pedersen,E.B. (2008) High physiological thermal triplex stability optimization of twisted intercalating nucleic acids (TINA). *Org. Biomol. Chem.*, **6**, 3714–3722.
19. Singh,S., Nielsen,P., Koshkin,A. and Wengel,J. (1998) LNA (locked nucleic acids): synthesis and high-affinity nucleic acid recognition. *Chem. Commun.*, 455–456.
20. Koshkin,A., Singh,S., Nielsen,P., Rajwanshi,R., Meldgaard,M., Olsen,C. and Wengel,J. (1998) LNA (locked nucleic acids): synthesis of the adenine, cytosine, guanine, 5-methylcytosein, thymine and uracil bicyclonucleoside monomers, oligomerization, and unprecedented nucleic acid recognition. *Tetrahedron*, **54**, 3607–3630.
21. Obika,S., Nanbu,D., Hari,Y., Andoh,J., Morio,K., Doi,T. and Imanishi,T. (1998) Stability and structural features of the duplexes containing nucleoside analogues with a fixed N-type conformation, 2′-O,4′- C-methyleneribonucleosides. *Tetrahedron Lett.*, **39**, 5401–5404.
22. Swayze,E.E., Siwkowski,A.M., Wancewicz,E.V., Migawa,M.T., Wyrzykiewicz,T.K., Hung,G., Monia,B.P. and Bennett,C.F. (2007) Antisense oligonucleotides containing locked nucleic acid improve potency but cause significant hepatotoxicity in animals. *Nucleic Acids Res.*, **35**, 687–700.
23. Braasch,D.A., Liu,Y. and Corey,D.R. (2002) Antisense inhibition of gene expression in cells by oligonucleotides incorporating locked nucleic acids: effect of mRNA target sequence and chimera design. *Nucleic Acids Res.*, **30**, 5160–5167.
24. Rapozzi,V., Cogoi,S. and Xodo,L.E. (2006) Antisense locked nucleic acids efficiently suppress BCR/ABL and induce cell growth decline and apoptosis in leukemic cells. *Mol. Cancer Ther.*, **5**, 1683–1692.
25. Stein,C.A., Hansen,J.B., Lai,J., Wu,S., Voskresenskiy,A., Hog,A., Worm,J., Hedtjarn,M., Souleimanian,N., Miller,P. *et al.* (2010) Efficient gene silencing by delivery of locked nucleic acid antisense oligonucleotides, unassisted by transfection reagents. *Nucleic Acids Res.*, **38**, e3.
26. Veedu,R.N. and Wengel,J. (2009) Locked nucleic acid as a novel class of therapeutic agents. *RNA Biol.*, **6**, 321–323.
27. Sapra,P., Wang,M., Bandaru,R., Zhao,H., Greenberger,L.M. and Horak,I.D. (2010) Down-modulation of survivin expression and inhibition of tumor growth in vivo by EZN-3042, a locked

nucleic acid antisense oligonucleotide. *Nucleosides Nucleotides Nucleic Acids*, **29**, 97–112.
28. Hansen,J.B., Fisker,N., Westergaard,M., Kjaerulff,L.S., Hansen,H.F., Thrue,C.A., Rosenbohm,C., Wissenbach,M., Orum,H. and Koch,T. (2008) SPC3042: a proapoptotic survivin inhibitor. *Mol. Cancer Ther.*, **7**, 2736–2745.
29. Guterstam,P., Lindgren,M., Johansson,H., Tedebark,U., Wengel,J., El Andaloussi,S. and Langel,U. (2008) Splice-switching efficiency and specificity for oligonucleotides with locked nucleic acid monomers. *Biochem. J.*, **412**, 307–313.
30. Roberts,J., Palma,E., Sazani,P., Orum,H., Cho,M. and Kole,R. (2006) Efficient and persistent splice switching by systemically delivered LNA oligonucleotides in mice. *Mol. Ther.*, **14**, 471–475.
31. Beane,R.L., Ram,R., Gabillet,S., Arar,K., Monia,B.P. and Corey,D.R. (2007) Inhibiting gene expression with locked nucleic acids (LNAs) that target chromosomal DNA. *Biochemistry*, **46**, 7572–7580.
32. Hu,J., Matsui,M., Gagnon,K.T., Schwartz,J.C., Gabillet,S., Arar,K., Wu,J., Bezprozvanny,I. and Corey,D.R. (2009) Allele-specific silencing of mutant huntingtin and ataxin-3 genes by targeting expanded CAG repeats in mRNAs. *Nat. Biotechnol.*, **27**, 478–484.
33. Ge,R., Heinonen,J.E., Svahn,M.G., Mohamed,A.J., Lundin,K.E. and Smith,C.I. (2007) Zorro locked nucleic acid induces sequence-specific gene silencing. *FASEB J.*, **21**, 1902–1914.
34. Ge,R., Svahn,M.G., Simonson,O.E., Mohamed,A.J., Lundin,K.E. and Smith,C.I. (2008) Sequence-specific inhibition of RNA polymerase III-dependent transcription using Zorro locked nucleic acid (LNA). *J. Gene Med.*, **10**, 101–109.
35. Beane,R., Gabillet,S., Montaillier,C., Arar,K. and Corey,D.R. (2008) Recognition of chromosomal DNA inside cells by locked nucleic acids. *Biochemistry*, **47**, 13147–13149.
36. Tolcher,A.W., Mita,A., Lewis,L.D., Garrett,C.R., Till,E., Daud,A.I., Patnaik,A., Papadopoulos,K., Takimoto,C., Bartels,P. *et al.* (2008) Phase I and pharmacokinetic study of YM155, a small-molecule inhibitor of survivin. *J. Clin. Oncol.*, **26**, 5198–5203.
37. Madsen,A.S., Kumar,T.S. and Wengel,J. (2010) LNA 5′-phosphoramidites for 5′®3′-oligonucleotide synthesis. *Org. Biomol. Chem.*, doi: 10.1039/C0OB00346H.
38. Geci,I., Filichev,V.V. and Pedersen,E.B. (2007) Stabilization of parallel triplexes by twisted intercalating nucleic acids (TINAs) incorporating 1,2,3-triazole units and prepared by microwave-accelerated click chemistry. *Chemistry*, **13**, 6379–6386.
39. Lundin,K.E., Hasan,M., Moreno,P.M., Tornquist,E., Oprea,I., Svahn,M.G., Simonson,E.O. and Smith,C.I. (2005) Increased stability and specificity through combined hybridization of peptide nucleic acid (PNA) and locked nucleic acid (LNA) to supercoiled plasmids for PNA-anchored 'Bioplex' formation. *Biomol. Eng.*, **22**, 185–192.
40. Paramasivam,M., Cogoi,S., Filichev,V.V., Bomholt,N., Pedersen,E.B. and Xodo,L.E. (2008) Purine twisted-intercalating nucleic acids: a new class of anti-gene molecules resistant to potassium-induced aggregation. *Nucleic Acids Res.*, **36**, 3494–3507.
41. Hojland,T., Kumar,S., Babu,B.R., Umemoto,T., Albaek,N., Sharma,P.K., Nielsen,P. and Wengel,J. (2007) LNA (locked nucleic acid) and analogs as triplex-forming oligonucleotides. *Org. Biomol. Chem.*, **5**, 2375–2379.
42. Hertoghs,K.M., Ellis,J.H. and Catchpole,I.R. (2003) Use of locked nucleic acid oligonucleotides to add functionality to plasmid DNA. *Nucleic Acids Res.*, **31**, 5817–5830.
43. Demidov,V., Frank-Kamenetskii,M.D., Egholm,M., Buchardt,O. and Nielsen,P.E. (1993) Sequence selective double strand DNA cleavage by peptide nucleic acid (PNA) targeting using nuclease S1. *Nucleic Acids Res.*, **21**, 2103–2107.
44. Zelphati,O., Liang,X., Hobart,P. and Felgner,P.L. (1999) Gene chemistry: functionally and conformationally intact fluorescent plasmid DNA. *Hum. Gene Ther.*, **10**, 15–24.
45. Egholm,M., Christensen,L., Dueholm,K.L., Buchardt,O., Coull,J. and Nielsen,P.E. (1995) Efficient pH-independent sequence-specific DNA binding by pseudoisocytosine-containing bis-PNA. *Nucleic Acids Res.*, **23**, 217–222.
46. Lundin,K.E., Ge,R., Svahn,M.G., Tornquist,E., Leijon,M., Branden,L.J. and Smith,C.I. (2004) Cooperative strand invasion of supercoiled plasmid DNA by mixed linear PNA and PNA-peptide chimeras. *Biomol. Eng.*, **21**, 51–59.
47. Thomson,J.B., Tuschl,T. and Eckstein,F. (1993) Activity of hammerhead ribozymes containing non-nucleotidic linkers. *Nucleic Acids Res.*, **21**, 5600–5603.
48. Rubin,E., Rumney,S.t., Wang,S. and Kool,E.T. (1995) Convergent DNA synthesis: a non-enzymatic dimerization approach to circular oligodeoxynucleotides. *Nucleic Acids Res.*, **23**, 3547–3553.
49. Veronese,F.M. and Morpurgo,M. (1999) Bioconjugation in pharmaceutical chemistry. *Farmaco*, **54**, 497–516.
50. Singh,Y., Murat,P. and Defrancq,E. (2010) Recent developments in oligonucleotide conjugation. *Chem. Soc. Rev.*, **39**, 2054.
51. Bonora,G.M., Drioli,S., Ballico,M., Faccini,A., Corradini,R., Cogoi,S. and Xodo,L. (2007) PNA conjugated to high-molecular weight poly(ethylene glycol): synthesis and properties. *Nucleosides Nucleotides Nucleic Acids*, **26**, 661–664.
52. Bonora,G.M., Ivanova,E., Zarytova,V., Burcovich,B. and Veronese,F.M. (1997) Synthesis and characterization of high-molecular mass polyethylene glycol-conjugated oligonucleotides. *Bioconjug. Chem.*, **8**, 793–797.
53. Zhao,H. (2008) Utility of Customized Targeted PEG linkers for the delivery of oligonucleotides without the use of transfection reagents. *Nanotechnology*, **2**, 372–374.